Non-Reciprocal MMIC-Based Dual-Band Bandpass Filters

Andrea Ashley#1 and Dimitra Psychogiou#\$*2

*Tyndall National Institute, Cork, Ireland

*Tyndall National Institute, Cork, Ireland

¹andrea.ashley@colorado.edu, ²D.Psychogiou@ucc.ie

Abstract-A new class of an RF front-end component that exhibits the co-designed function of a dual-band bandpass filter and an RF isolator is presented. The proposed non-reciprocal dual-band bandpass filter (NDBPF) is based on two multiresonant cells and one non-reciprocal resonant stage. By cascading them in series, a dual-band transfer function—shaped by four poles (two for each passband) and six transmission zeros—is created in the forward direction and full RF signal cancellation is obtained in the reverse one. For proof-of-concept demonstration purposes, a NDBPF prototype was designed at X-band and manufactured with a commercially-available MMIC GaAs process. It exhibited two bands with the following RF measured characteristics: center frequencies: 8.33 GHz and 10.17 GHz, 3-dB fractional bandwidth: 6.4% and 3.6%, maximum gain: 6.38 dB and 0.3 dB, and isolation >36.7 dB and 19.5 dB at respectively the lower and upper band.

Keywords—Bandpass filter, co-design, gain, isolation, MMIC filter, MMIC isolator, non-reciprocal.

I. INTRODUCTION

Full-duplex RF front-ends have long been sought for a wide range of wireless communication and radar systems due to their potential in using the same frequency for the transmit and the receive operation. However, their practical development has been hindered by the lack of compact antenna front-end interfaces that could effectively isolate the transmit and the receive modules of their RF front-ends. Existing isolation solutions using simultaneous transmit and receive (STAR) antennas [1] or ferrite-based circulators and isolators [2] are prohibitively large. Whereas STAR antennas require multiple and widely-spaced elements, ferrite-based components are in need for external magnetic biasing which makes them not suitable for IC integration. Size constraints become even more critical when multiple bands or functions need to be supported by the RF front-end. In this case, multiple off-chip bandpass filters (BPFs) need to be integrated to suppress the spurious signals from the power amplifier (PAs) and the interference that would otherwise saturate the low noise amplifier (LNA).

Miniaturization of the full-duplex RF front-ends is mostly aimed at the RF component level. For example, compact RF isolators have been developed by incorporating transistor-based networks with RF couplers [3] and by cascading LNAs with attenuators [4]. However, these approaches exhibit moderate levels of insertion loss (IL) (\sim 1.5-2.5 dB) and high RF power consumption ($P_{DC} > 68$ mW in [4]). RF co-design concepts where the isolator function and the BPF are incorporated within the volume of the same RF component have also being explored as an effective miniaturization mechanism. These non-

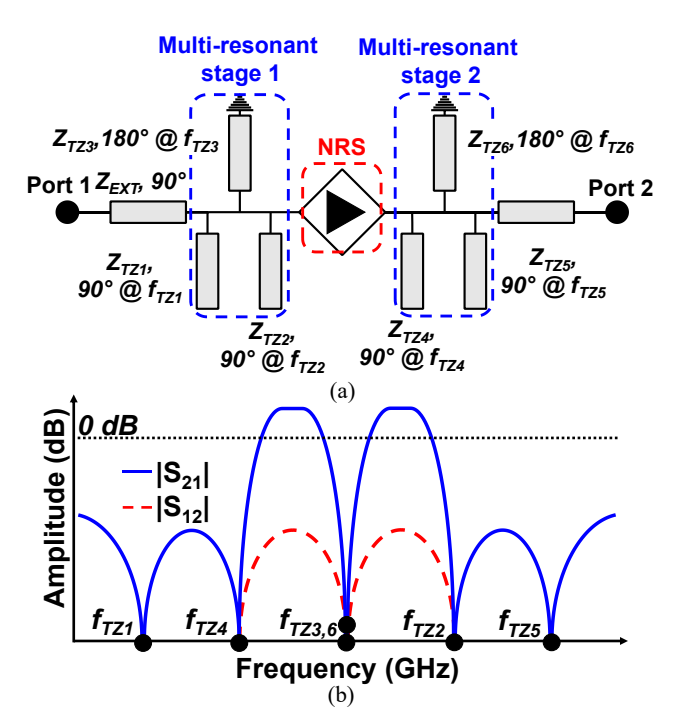


Fig. 1. NDBPF. (a) Block diagram that consists of two multi-resonant stages and one NRS. (b) Conceptual S-parameter response of the NDBPF.

reciprocal bandpass filters (NBPFs) are implemented by: i) coupled-resonator-based configurations where the non-reciprocal filtering function is obtained by using non-reciprocal transistor-based resonators [5] and by ii) breaking the time-reversal symmetry in the BPF by modulating the resonant frequency of the resonators through spatio-temporal modulation (STM) [6]-[8]. However, both of these concepts are implemented with off-chip components which make them large in size. Furthermore, the STM-based NBPF concepts, are only suitable for low frequency realizations (<1 GHz) due to their modulation frequencies need to be approximately equal to the passband bandwidth. Furthermore, they suffer from high levels of IL (3.7-5.5 dB) and low levels of isolation (6.2 dB in [6]).

Considering the aforementioned limitations, this manuscript presents a new class of IC integrated non-reciprocal bandpass filters (NDBPFs) using a commercially-available GaAs MMIC process. In particular, we demonstrate a new RF design concept in which multi-resonant stages that each create two poles and three transmission zeros (TZs) are combined with a non-reciprocal stage (NRS) for the realization of a quasi-

elliptic-type dual-band transfer function in the forward direction and high levels of IS in the reverse one.

II. THEORETICAL FOUNDATIONS

The circuit details and operating principles of the NDBPF concept are shown in Fig. 1. It is based on a NRS and two multi-resonant stages. Whereas the NRS creates a non-reciprocal power transmission response, each of the multi-resonant stages results in a dual-band reciprocal transfer function that is shaped by two-poles and three TZs. Thus, the forward direction of the two-port network, exhibits a dual-band transfer function with two passbands shaped by four poles (two in each band) and six TZs.

To better illustrate the operational characteristics of the NDBPF, Figs. 2-4 demonstrate the circuit schematic and ideal S-parameter response of the NRS, the multi-resonant stage and the overall NDBPF. In particular, the NRS is based on a directional coupler and a non-reciprocal RF signal path that is connected between the through- and reverse-coupled ports of the coupler—shaped by two pairs of 90°-long transmission lines (TLs) at f_{cen} (10 GHz in this example) with characteristic impedances Z_A and Z_B and coupling factor k, (1)—. The nonreciprocal RF signal path comprises a transistor-based element which typically exhibits finite gain and isolation levels and additional phase-control elements (i.e., TLs with characteristic impedance Z_C and 90°-long at f_{cen}). By appropriately selecting k (1) and Z_0 , the NRS can be designed to exhibit higher gain than the transistor-based element and ideally infinite isolation at f_{cen} , as shown in Fig. 2 for the example case of a transistorbased element with finite isolation characteristics. Furthermore,

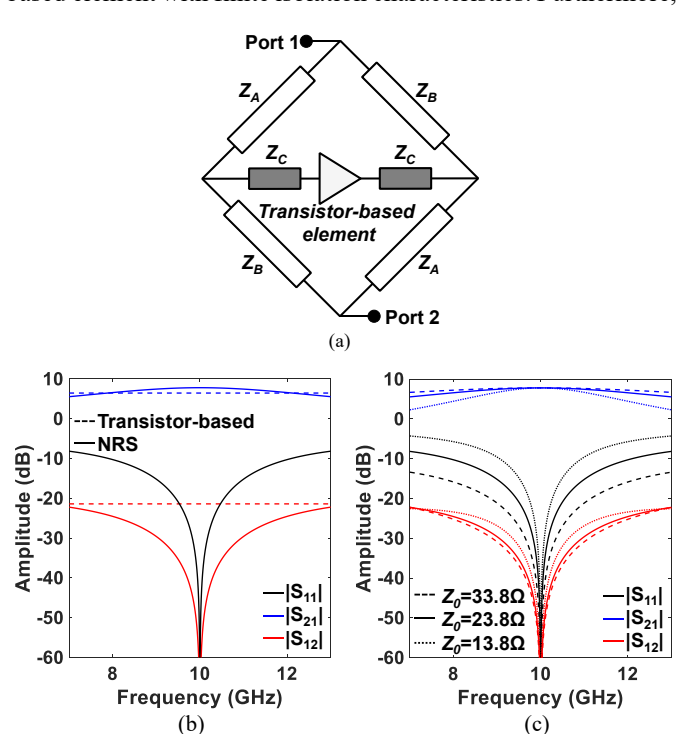


Fig. 2. (a) Block diagram for the NRS. (b) Ideal power transmission ($|S_{21}|$), isolation ($|S_{12}|$), and reflection ($|S_{11}|$) response of the NRS (solid lines) and its corresponding transistor-based element (dashed lines). The coupler characteristics are: $Z_0 = 23.8 \,\Omega$, k = 0.0072, Transistor S-parameters: $S_{11} = 0$, $S_{12} = 0.085$, $S_{21} = 2.1$, and $S_{22} = 0$. (c) Varying BW by changing Z_0 .

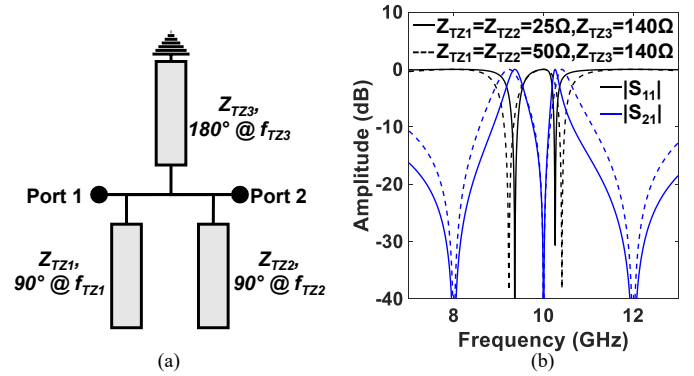


Fig. 3. Multi-resonant stage. (a) Circuit schematic. (b) Ideal power transmission $(|S_{21}|)$ and reflection $(|S_{11}|)$ response with varying impedance.

the operational BW of the NRS can be altered by changing Z_0 as shown in Fig. 2(c).

$$Z_A = Z_0 \sqrt{1 - k}; \ Z_B = Z_0 \sqrt{(1 - k)/k}; \ Z_C = Z_0$$
 (1)

The circuit details and operational characteristics of the multi-resonant stage are shown in Fig. 3. It consists of three stubs—two 90°-long open-ended and one 180°-long shortcircuited stub—that result in two passbands in-between three TZs [9]. Each of the TZs is located at the resonant frequency of its corresponding stub and the center frequencies of the passbands are controlled by their characteristic impedances [see Fig. 3(b)]. By combining multiple multi-resonant stages with the NRS, high-order dual-band transfer functions with enhanced power transmission response and high isolation can be obtained. This is shown in Fig. 4 for the example case of a NDBPF that comprises two multi-resonant stages and one NRS and exhibits two passbands in-between six TZs. The TZs of the multi-resonant stages can be placed at identical or different frequencies with the purpose of enhancing the out-of-band suppression bandwidth as shown in Figs. 4(a), (b) respectively. The overall gain and isolation at each passband, is determined by the NRS and is equal to the NRS's gain and isolation at the frequencies where the passbands are set. Therefore, in order to achieve higher gain and isolation levels than the transistorbased element, the passbands would need to be designed in the

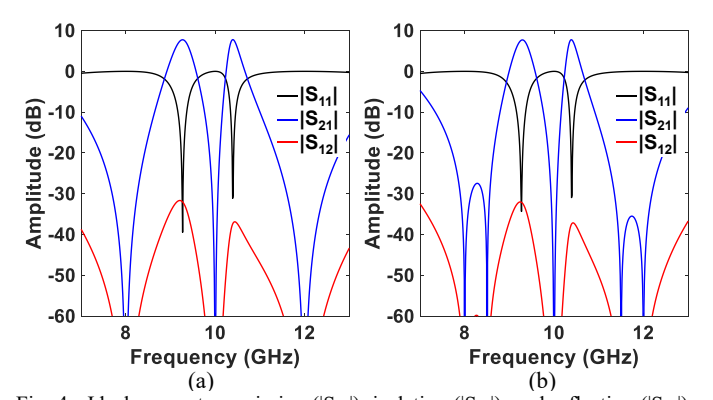


Fig. 4. Ideal power transmission ($|S_{21}|$), isolation ($|S_{12}|$), and reflection ($|S_{11}|$) response of the NDBPF with (a) identical multi-resonant stages and (b) dissimilar multi-resonant stages. In these examples: $Z_0 = 23.8 \ \Omega$, k = 0.0072, Transistor S-parameters: $S_{11} = 0$, $S_{12} = 0.085$, $S_{21} = 2.1$, and $S_{22} = 0$.

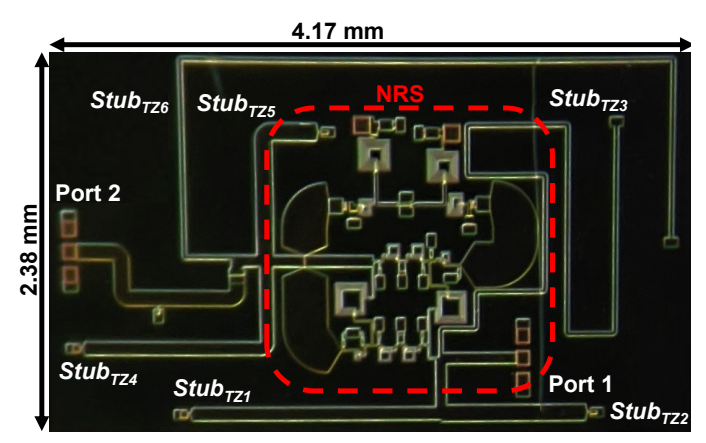


Fig. 5. Photograph of the proposed NDBPF. The NRS is boxed in red and the TZs are denoted by the white labels.

frequency range where the NRS gives higher gain and isolation than the transistor-based element. For example, between 7.9 to 12.1 GHz for the design case shown in Fig. 2(b).

III. EXPERIMENTAL VALIDATION

To evaluate the validity of the NDBPF concept, a dual-band X-band prototype with two bands centered at 8.6 GHz and 10.4 GHz was designed and manufactured using a commercially available GaAs PIH1-10 process. A photograph of the manufactured prototype is shown in Fig. 5 with the stubs for each TZ and NRS labelled. The NDBPF design was performed as follows. At first a two-finger pHEMT transistor (biased with $V_D=3V$ and $V_G=0.95V$) with resistive matching networks at the gate and the drain (added for stability and impedance match), is selected to provide 4-10.8 dB of gain at X-band. The transistorbased element is then embedded in the NRS. The NRS is designed for a gain of 9.4 dB at 9.4 GHz and as such its TLs are selected as follows: $Z_A=23.5\Omega$, $Z_B=140\Omega$ and $Z_C=27\Omega$, $Z_0=23.8\Omega$. In an effort to keep the size of the NDBPF small, the NRS coupler was implemented through lumped-element (LE)based TLs. The TLs connecting the coupler to the transistorbased element were implemented using both microstrip (designed on Metal layer 1) and LE configurations. The multiresonant stages were then added to the input and output of the NRS (using TLs designed on Metal layer 2 to prevent overlap with the NRS) with the purpose of achieving 6 TZs at 7.3, 12.2, 9.8, 6.4, 13, and 9.8 GHz and widening the out-of-band suppression bandwidth. Capacitively-loaded stubs were used for size compactness and their impedances were selected as

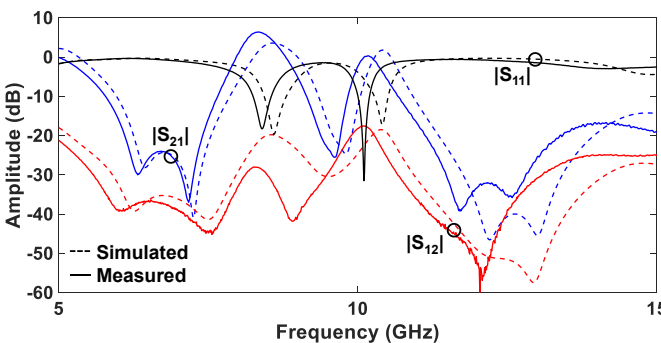


Fig. 6. EM-simulated and measured S-parameters for the prototype in Fig. 5.

Table 1. Comparison with state-of-the-art NBPFs

| | Ref. | Topology | fcen (GHz) | IS (dB) | S ₂₁ (dB) | No. of Bands | |
|---|------|------------|---------------|-----------|---------------------------|-----------------|-------------|
| | [5] | Microstrip | 2.2 | 44 | +5.6 | 1 | 39.2 x 48 |
| | [6] | STM | 1 | 6.2 | -5.5 | 1 | 20.7 x 18.3 |
| | [7] | STM | 1.175 | 28 | -4.5 | 1 | N/A |
| | [8] | STM | 0.14 | 52.8 | -3.7 | 1 | N/A |
| ſ | This | GaAs | 8.33, | 36.7,19.5 | +6.38, | 2 | 2.38 x 4.17 |
| L | work | MMIC | 10.17 | 30.7,19.3 | +0.3 | | 2.36 X 4.17 |

follows: $Z_{TZI} = Z_{TZ4} = 46\Omega$, $Z_{TZ2} = Z_{TZ5} = 40\Omega$; shorted 180°-long stubs were selected for the TZs in between the bands and their impedances were as follows: $Z_{TZ3} = Z_{TZ6} = 72\Omega$.

The measured RF performance of the NDBPF was characterized in terms of S-parameters and is shown in Fig. 6. A comparison with the EM-simulated S-parameters is also provided which as shown are in a fair agreement. The observed differences in the passband gain and the location of the TZs are attributed to process manufacturing variations that led to the TZs in the measured response to move to lower frequencies. The RF measured characteristics for this bias state (V_D=3V, and V_G=0.95V) are summarized as follows: center frequencies: 8.33 GHz and 10.17 GHz, 3-dB fractional bandwidth (FBW): 6.4% and 3.6%, maximum in-band gain: 6.38 dB and 0.3 dB and isolation > 36.7 dB and 19.5 dB. A comparison with stateof-art NBPFs is provided in Table 1. As shown, this is the only GaAs NBPF with dual-band capability and gain in its power transmission response, while it exhibits significantly smallest size and higher operational frequency than the NBPFs in [5]-[8].

IV. CONCLUSION

This paper reported on the RF design and experimental testing of a NDBPF using a commercially-available GaAs MMIC process. The proposed concept uses as basis cascaded NRSs and multi-resonant stages. Whereas the non-reciprocal transfer function characteristics are inherited by the NRS, the dual-band behavior is attributed to the multi-resonant stages that create two passbands in-between six TZs. The operating principles of the NDBPF were presented through linear simulations and the design and testing of an experimental prototype at X-band.

ACKNOWLEDGMENT

This work has been supported in part by the National Defense Science and Engineering Graduate (NDSEG) Fellowship and the National Science Foundation under Grant ECCS-1941315. We would like to thank WIN Semiconductors Corp. for providing access to their PIH1-10 process and for manufacturing the MMIC components.

REFERENCES

- [1] K. Lu, C. Goodbody, T. Karacolak and N. Tran, "An interior parasitic patch antenna with wide isolation bandwidth for simultaneous transmit and receive (STAR)," 2019 IEEE Int. Symp. on Antennas and Propag. and USNC-URSI Radio Science Meeting, Atlanta, GA, USA, 2019, pp. 1513-1514.
- [2] M. F. Farooqui, A. Nafe and A. Shamim, "Inkjet printed ferrite-filled rectangular waveguide X-band isolator," 2014 IEEE MTT-S Int. Microw. Symp. (IMS), Tampa, FL, 2014, pp. 1-4.

- [3] Jen-Feng Chang, Jui-Chih Kao, Yu-Hsuan Lin and Huei Wang, "A 24-GHz fully integrated isolator with high isolation in standard RF 180-nm CMOS technology," 2014 IEEE MTT-S Int. Microw. Symp. (IMS2014), Tampa, FL, 2014, pp. 1-3.
- [4] M. F. Cordoba-Erazo and T. M. Weller, "A 1.4 GHz MMIC active isolator for integrated wireless systems applications," WAMICON 2014, Tampa, FL, 2014, pp. 1-3.
- [5] A. Ashley and D. Psychogiou, "Non-reciprocal RF-bandpass filters using transistor-based microwave resonators," 2019 49th Eur. Microw. Conf. (EuMC), Paris, France, 2019, pp. 603-606.
- [6] X. Wu, M. Nafe, A. A. Melcón, J. Sebastián Gómez-Díaz and X. Liu, "A non-reciprocal microstrip bandpass filter based on spatio-temporal modulation," 2019 IEEE MTT-S Int. Microw. Symp. (IMS), Boston, MA, USA, 2019, pp. 9-12.
- [7] M. Pirro, C. Cassella, G. Michetti and M. Rinaldi, "Low loss non-reciprocal filter for miniaturized RF-front-end platforms," 2019 Joint Conf. of the IEEE Int. Freq. Control Symp. and Eur. Freq. and Time Forum (EFTF/IFC), Orlando, FL, USA, 2019, pp. 1-3.
- [8] D. Simpson and D. Psychogiou, "Magnet-less non-reciprocal bandpass filters with tunable center frequency," 2019 49th Eur. Microw. Conf. (EuMC), Paris, France, 2019, pp. 460-463.
- [9] C. Quendo, A. Manchec, Y. Clavet, E. Rius, J. Favennec and C. Person, "General synthesis of N-band resonator based on N-order dual behavior resonator," in *IEEE Microw. and Wireless Compon. Lett.*, vol. 17, no. 5, pp. 337-339, May 2007.